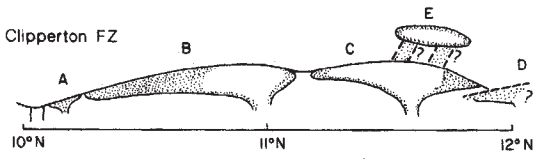

Fig. 4 Five magma types observed along EPR axis 10°-12° N. Dotted areas indicate >8% mineral phenocrysts. Magma type E is presumed to be an off-axis (4 km) seamount from which lavas have intruded into the axial region at two locations. It is uncertain whether magma type D is a unique magma batch like magma type A, near the propagating rift tip, or the proximal tip of a down-axis injection from a magma chamber near 12°30′ at the next axial topographic high.

at two localities on the second topographic high. A previous cruise by the French *N.O.J. Charcot*[7] in the same general area also recovered samples of E-MORB from the axial graben and from the eastern rim of the axis near 11°27′ N. We recovered two samples about 20 km away in the northern part of the axis approaching the tip of the west limb of the OSC. R. Hekinian provided splits of the French samples which we analysed; these are E-MORBs similar to those we recovered. The type E lavas have higher Ti and lower Fe content for a given MgO concentration compared with the other axial lavas. They have very high concentrations of incompatible elements such as K, Sr, Zr and Nb, and higher Zr/Y and lower Zr/Nb ratios than the other magma types. The *Charcot* surveys have shown that at this latitude, about 11°45′ N, there is a large seamount only about 4 km to the west of the ridge axis which is erupting various types of lavas (R. Hekinian, personal communication). Available data are not sufficient to determine whether lavas from this seamount may have been injected transversely, or whether they flowed on the sea floor from the seamount to the present EPR axis.

Conclusion

Figure 4 shows diagrammatically the distribution of the five magma types. Our observations support the Francheteau–Ballard model of axial processes. We suggest that the topographic highs are the locus of magma upwelling into magma chambers, and that magmas are injected down the axes from these localities. These lavas show systematic changes in composition along the axis. In essence, the EPR is made up of a series of volcanoes separated by transform or non-transform (OSC) offsets. This is analagous to the observations of central volcanoes located along the rift zone in Iceland which have been shown to inject magma, subcrustally, up to 70 km along rifts from the central volcano; this injection often is highly asymmetric as in these EPR examples[12].

We have shown that the depression between the overlapping limbs of an OSC is old and inactive. We have demonstrated that the eastern limb of the OSC at 11°45′ N is very active and propagating southward. Our data indicate that lavas at the propagating tip of an overlapping pair of rifts, or close to a large transform, may have distinct chemical compositions. Our observations also suggest local chemical heterogeneity in the mantle that must give rise to the pronounced differences between axial and nearby seamount lavas. We also observe small-scale mantle heterogenity or differences in melt formation, local plumbing or magma mixing that give rise to the distinct compositions observed between individual magma centres or volcanoes along axis. These differences are superimposed on compositional variation which can be produced by the fairly extensive fractionation which has occurred within each magma batch. Further aspects of these differences and the nature of the source regions are currently being investigated by isotope and rare-earth element analysis and geochemical modelling. Although a variety of magma compositions have been noted in samples recovered previously from the EPR, this is the first documentation of systematic variation in lava composition and morphology that can be ascribed to specific axial processes and their relative position in time and space.

We thank the officers, crew and technicians of R/V *Melville* for assistance, and Rob Zierenberg (USGS) for help in dredging. We thank Brian Schroeder, Margaret Sulanowska and Tim O'Hearn for help in the analysis of the samples. J. Marsh and M. Harvey typed the manuscript. The manuscript benefitted from reviews by R. Hekinian. This work was supported by NSF grant OCE83-09977. This is contribution no. 5962 from the Woods Hole Oceanographic Institution.

Received 21 June; accepted 30 September 1985.

1. Macdonald, K. & Fox, P. J. *Nature* **302**, 55-58 (1983).
2. Schouten, H. & Klitgord, K. D. *Nature* **303**, 549-550 (1983).
3. Lonsdale, P. *Bull. geol. Soc. Am.* **96**, 313-327 (1985).
4. Francheteau, J. & Ballard, R. D. *Earth planet. Sci. Lett.* **64**, 93-116 (1983).
5. Macdonald, K., Sempere, J. C. & Fox, P. J. *J. geophys. Res.* **89**, 6049-6069 (1984).
6. Ballard, R. D., Hekinian, R. & Francheteau, J. *Earth planet. Sci. Lett.* **69**, 176-186 (1984).
7. Hekinian, R., Francheteau, J. & Ballard, R. D. *Oceanol. acta* **8**, 147-155 (1985).
8. Hekinian, R. *et al. Science* **219**, 1321-1324 (1983).
9. McConachy, T. F., Mottl, M. J. & Von Herzen, R. P. *EOS* **65**, 1124 (1984).
10. Lonsdale, P. *J. geophys. Res.* **88**, 9393-9406 (1983).
11. Langmuir, C. H. & Bender, J. F. *Earth planet. Sci. Lett.* **69**, 107-127 (1984).
12. Sigurdsson, H. & Sparks, S. R. J. *Nature* **274**, 126-130 (1978).
13. Sinton, J. M., Wilson, D. S., Christie, D. M., Hey, R. N. & Delaney, J. R. *Earth planet. Sci. Lett.* **62**, 193-207 (1983).
14. Phillips, J. D., Driscoll, A. H. J., Peal, K. R., Marquet, W. M. & Owen, D. M. *Deep-Sea Res.* **26**, 211-225 (1979).
15. Schroeder, B., Thompson, G., Sulanowska, M. & Ludden, J. N. *X-ray Spectrom.* **9**, 198-205 (1980).
16. Melson, W. G. *et al. Smithson. Contr. Earth Sci.* **19**, 31-60 (1977).

Patterns of *engrailed* and *fushi tarazu* transcripts reveal novel intermediate stages in *Drosophila* segmentation

Michael P. Weir & Thomas Kornberg

Department of Biochemistry and Biophysics, University of California, San Francisco, California 94143, USA

Transcripts of the engrailed *and* fushi tarazu *genes in young* Drosophila *embryos are initially patterned in intervals larger than a single segment. The segmental pattern evolves in a stepwise sequence through successively smaller spatial units.*

THE *Drosophila* embryo is spatially organized into repeating units—the anterior and posterior developmental compartments[1] of each metameric segment. These compartment types alternate in a striking zebra-like pattern as transverse encircling bands of cells on the surface of the young embryo[2,3]. Their presence is not apparent from the embryo morphology, but is revealed by cell lineage studies[4-6], and by *in situ* identification of cells that express the *engrailed* locus. The *engrailed* locus is expressed only in the posterior compartment cells[2].

The *engrailed* gene is one of a number of genes whose function

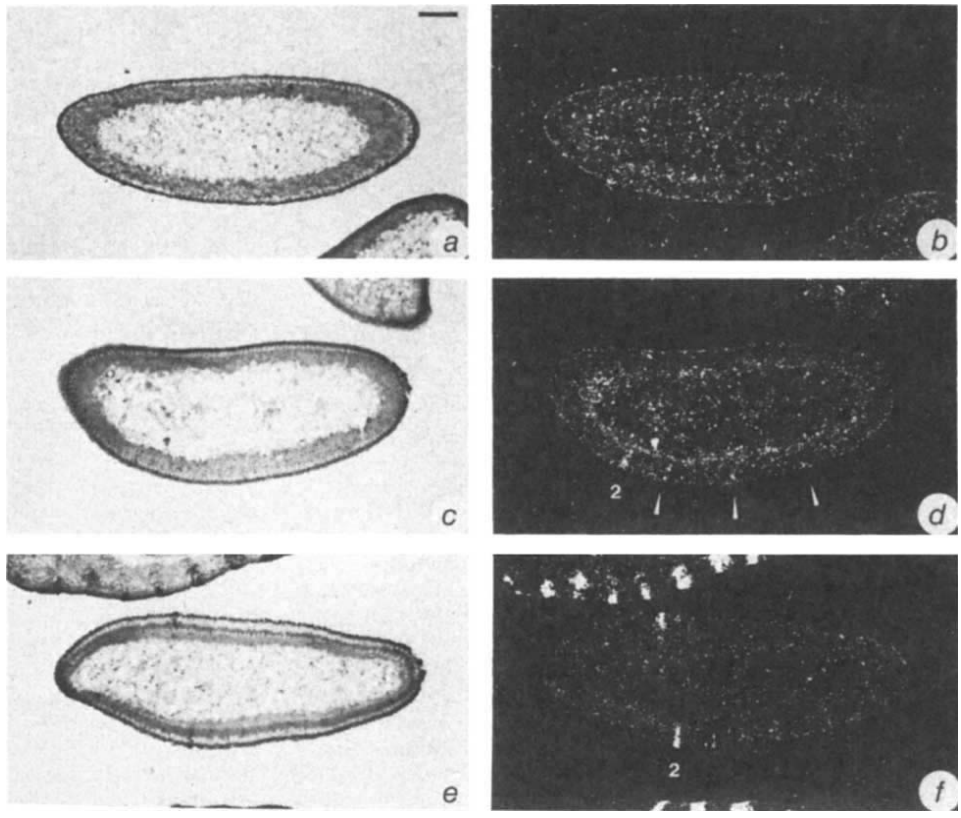

Fig. 1 Micrographs showing *engrailed* transcripts in blastoderm stage embryos. Bright-field (left) and corresponding dark-field (right) micrographs were recorded after hybridization with an *engrailed* cDNA probe and autoradiography. Sections in all figures are oriented anterior left. *a, b,* Section of embryo at nuclear cycle 13 with no detectable localization of autoradiographic grains. *c, d,* Early cycle 14 embryo, oriented ventral down, with nuclei beginning to elongate. Ten such sections were found with grains most prominently over the nuclei that later will correspond to the second of the 14 stripes (Fig. 2*f*). In this section, sparse concentrations of grains are also over the nuclei of what are probably stripes 4, 8 and 12 (arrowheads). *e, f,* Horizontal section. The nuclei have elongated and membrane furrows have extended into the cytoplasm just beyond the nuclei. A prominent autoradiographic signal is over the nuclei and cytoplasm of stripe 2. Scale bar, 50 μm.

Methods. Embryos were dechorionated with 2.5% sodium hypochlorite for 3 min, fixed in 2% paraformaldehyde, 0.5× phosphate-buffered saline (PBS) and 50% *n*-heptane for 15 min using vigorous shaking, and transferred to 45% methanol, 25 mM EGTA, 50% heptane and shaken on dry ice for 10 min. Vitelline membranes were then removed by rapid heating to 40 °C[27]. Following three washes in 90% methanol, 50 mM EGTA, embryos were transferred in stages to PBS, before embedding in O.C.T. (Miles Scientific) using liquid nitrogen. *In situ* hybridizations onto 8 μm frozen sections were performed as described previously using tritiated nick-translated DNA probes of the p9-1.4 cDNA[2]. Embryonic stages: Observation during nuclear cycles 10–13, syncytial blastoderm stages, shows that at cycle 10, yolk nuclei stop dividing, pole cells bud from posterior end, and remaining nuclei appear on the surface and divide in near synchrony. At cycle 14, cellular blastoderm stage, there is a ~90 min period of mitotic quiescence during which membranes form between the peripheral nuclei and gastrulation begins. Embryos in the sections were staged by counting nuclei in 100-μm intervals along the embryo periphery. 43 measurements of cycle 14 embryos yielded a value of 15.6 ± 1.4 nuclei per 100 μm. The values used for other stages were: cycle 10, 4 nuclei; cycle 11, 6 nuclei; cycle 12, 8 nuclei; and cycle 13, 11 nuclei.

is essential for segmentation. The gene *fushi tarazu* (*ftz*) is another[7], and it is expressed in the young embryo in seven evenly spaced bands of cells with a two-segment periodicity[8]. Although each band has the width of one segment[9], the spatial relationship between the bands of *ftz*-expressing cells and the metameric segments is not known. Nevertheless, the expression of *engrailed* and *ftz* both provide indications of the timing and nature of the processes that subdivide the embryo into equal-sized metameres, and they provide molecular markers that can be used to follow the process of segmentation.

In this study, the generation of the *engrailed* and *ftz* patterns of expression have been determined by *in situ* hybridization. The use of fixation methods that better preserve the morphology of the early *Drosophila* embryo and longer autoradiographic exposures have yielded a more precise portrayal of the generation of the segmental patterns and have revealed several new aspects of segmentation. Transcription patterns for both *engrailed* and *ftz* suggest that subdivision of the embryo proceeds through a sequence of intermediate stages, each stage part of a process that partitions the embryo into progressively smaller units.

Expression of *engrailed* in early embryos

After fertilization and nine synchronous mitotic divisions, three types of nuclei can be distinguished in the *Drosophila* (cycle 10) embryo: approximately 100 centrally located yolk nuclei, about 450 peripheral nuclei at the embryo surface that will generate the somatic tissues, and about 12 future germ cells at the posterior pole[10–14]. Four divisions of the peripheral nuclei follow. During the 14th cell cycle, the nuclei, initially round, elongate before membrane furrows invaginate from the surface of the embryo to separate the nuclei into individual cells[15]. During this period the nuclei become highly active in transcription[16,17] (A description of relevant embryonic stages is given in Fig. 1 legend.)

To identify nuclei that express the *engrailed* locus, wild-type embryos were fixed and quick-frozen for preparation of cryostat sections. After hybridization with radiolabelled probes generated from an *engrailed* cDNA clone[2], autoradiographs were exposed for 3–4 months to detect *engrailed* transcripts. Sections from embryos younger than stage 14 did not have grains localized either over nuclei or in any other distinctive pattern (Fig. 1*a, b*), yet the grain density over such embryos was consistently higher than background. Since Northern blot analysis of RNA isolated from cleavage stage and syncytial blastoderm stage embryos has revealed the presence of *engrailed* transcripts[18], these early transcripts are either not regionally localized or our *in situ* hybridization methods lacked sufficient sensitivity for definitive detection.

As the embryo matures through the 14th division cycle, striking changes in *engrailed* expression produce a pattern of 14 equally spaced and equally dense stripes (Fig. 2*f*). The pattern is generated in a reproducible and recognizable sequence. Anterior bands appear before posterior ones, ventral bands before dorsal ones (Figs 1, 2). However, superimposed on this anterior to posterior sequence of appearance are strong but transient periodicities in the density of autoradiographic grains over the different bands: (1) the first two prominent bands in the ventral region are bands 2 and 8; (2) bands 4 and 8 become prominent before band 6, and band 12 before 10, suggesting a

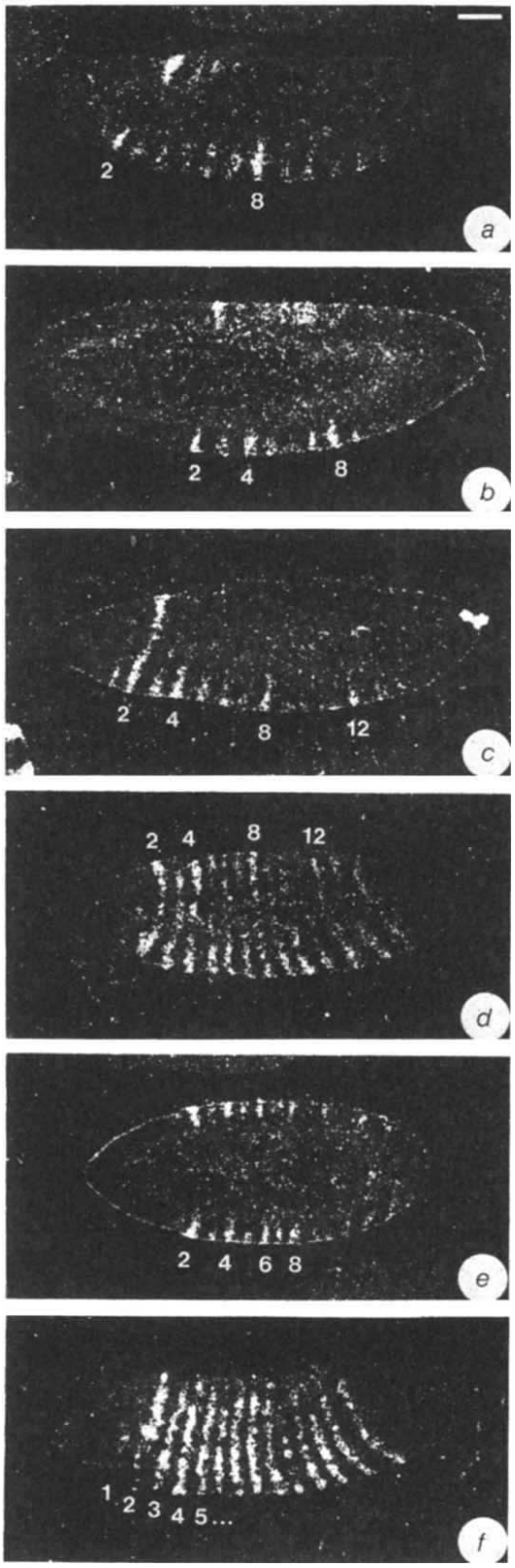

Fig. 2 Micrographs of *engrailed* transcripts in early gastrulas. Dark-field micrographs of embryos oriented ventral down except for *e*, a horizontal section. Stripes are more prominent in the anterior and ventral portions. Most prominent stripes are: *a*, ventral 2 and 8, dorsal 2; *b*, ventral 2, 4 and 8, dorsal 2; *c*, ventral 2, 4, 8 and 12, dorsal 2; *d*, ventral 2–14 and dorsal 2, 4, 8 and 12; *e*, lateral 2, 4, 6, 8, 10, 12; *f*, all stripes approximately equal. Note that among the weak stripes between 4 and 8 in *b*, stripe 6 is the weakest. *a* Has a two-band pattern, *b–d*, four-segment periodicity, and *e*, a two-segment periodicity. Scale bar 50 μm.

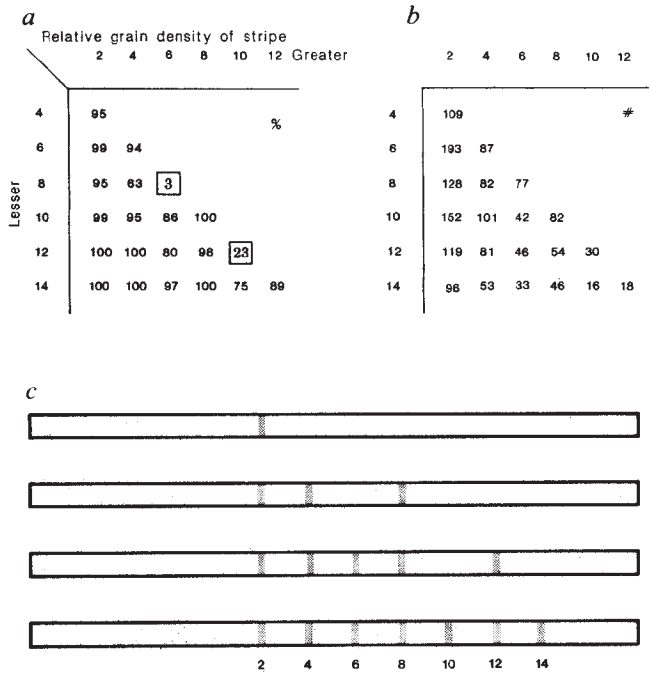

Fig. 3 The order of appearance of the even-numbered bands of *engrailed* hybridization was determined in 247 section edges from 132 sections of 105 different embryos. Section edges chosen for examination were those with clear differences in band intensities. After a pairwise comparison of each of the even-numbered bands, only cases of clear intensity differences were tabulated. *b*, Total number of instances in which two bands with different intensities were compared; *a*, the percentage of such comparisons in which the bands designated along the horizontal axis were more intense than those indicated on the vertical axis. The boxed numbers indicate cases of posterior stripes appearing before anterior ones: 8 before 6 and 12 before 10. *c*, A summary of the types of patterns that were observed. Embryos of increasing age are portrayed as rectangles with their posterior pole to the right. The dotted areas indicate bands of hybridization.

four-segment reiterated pattern; and (3) when all of the even-numbered bands become prominent, they have autoradiographic signals that are briefly stronger than those of the intervening odd-numbered bands, suggesting a two-segment reiterated pattern. A detailed description of this progression follows.

The first of the prominent bands of hybridization was observed in early cycle 14 embryos whose nuclei had just initiated the elongation process (Fig. 1*c*, *d*). A stripe of grains with a width of one to two nuclei was oriented perpendicular to the long axis of the embryo, about one-third from the anterior end. Grain density was initially greater over the nuclei than over the adjacent cytoplasm (Fig. 1*c*, *d*), but during the 14th cycle, the relative proportion of cytoplasmic grains increased (Fig. 1*e*, *f*). With the commencement of gastrulation near the end of cycle 14, the stripe of hybridization was at the posterior edge of the cephalic furrow, and corresponded to the second of the 14 stripes from the anterior end (Fig. 2*f*). The posterior edge of the cephalic furrow is the position of the mandibular or maxillary head segment primordium[9,19].

The fourth and eighth bands, weak concentrations of grains at the beginning of cycle 14 (Fig. 1*c*, *d*), were (along with band 2) consistently the most intense as gastrulation began (Fig. 2*a–d*). The relative strengths of the autoradiographic signals over the fourth and eighth stripes were often unequal (82 cases). In such sections in which the ventral and dorsal surfaces could be unambiguously identified, band 4 was more intense than band 8 dorsally (19/19 cases), and band 8 was more intense ventrally (13/16 cases) (Fig. 2*a*). Thus, ventrally, band 8 appeared before 4, and dorsally, band 4 appeared before 8. Band 12 was also observed as a prominent early autoradiographic signal (Fig. 2*c*, *d*), although with less regularity.

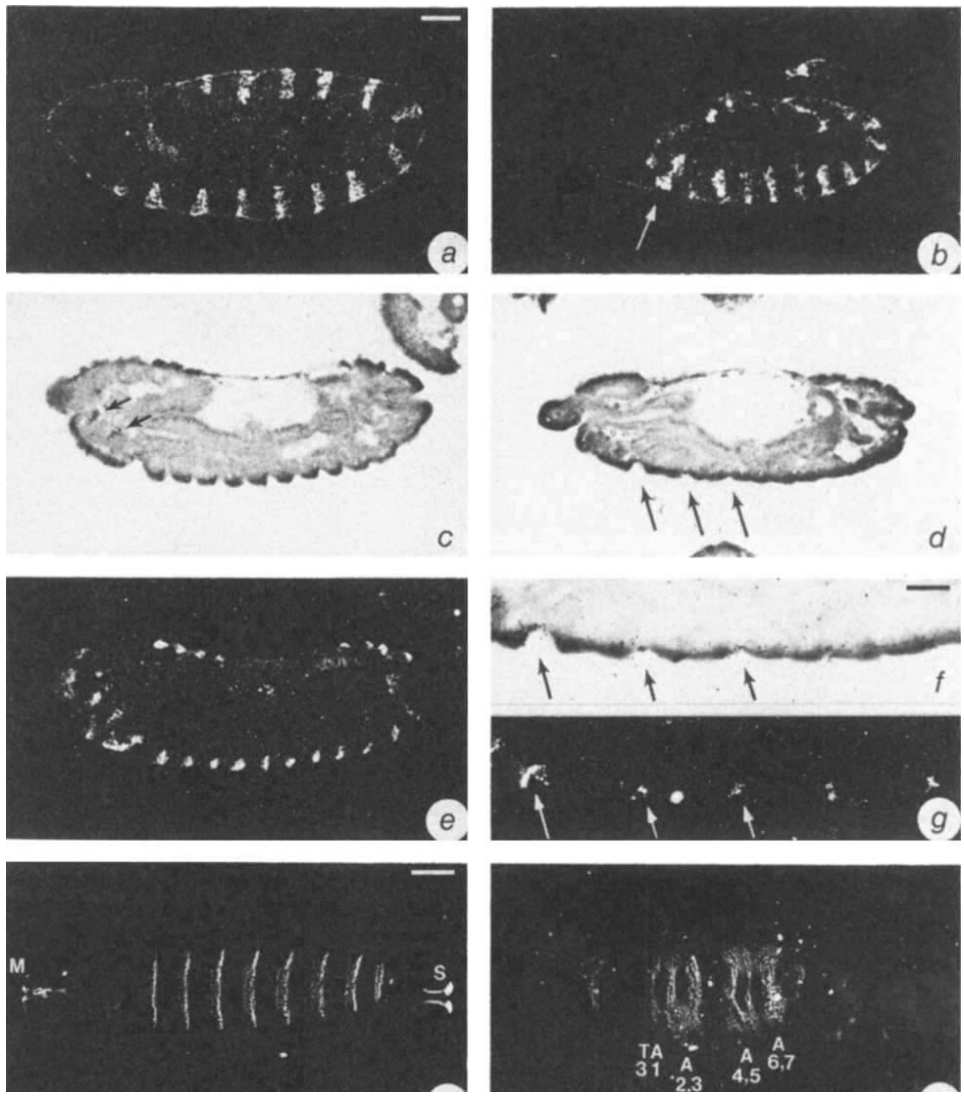

Fig. 4 Micrographs of *engrailed* transcripts in *engrailed* mutants. *a*, Dark-field micrograph of a section of a gastrulating wild-type embryo. The grains of adjacent stripes are approximately equal in density (also see Fig. 2*f*). *b*, Dark-field micrograph of a section of an en^{C2}/en^{SF31} mutant embryo during germ-band elongation (en^{SF31} deletes the entire *engrailed* locus). Signal alternates in strength in adjacent segments and the phasing is the same as observed in younger wild-type embryos: prominent stripe 2 is located in the posterior part of the cephalic furrow (arrow). *c*, *e*, Bright-field and dark-field images of a wild type embryo following germ-band shortening. The signal strengths are approximately equal over adjacent segments. Note the grains over the anterior portion of the ventral nerve chord (arrows in *c*). Serial sections of the embryo revealed labelling over the other ventral nerve chord ganglia. Such expression is consistent with earlier reports that *engrailed* function is essential in the adult nervous system[28]. *d*, Bright-field micrographs of a section of an en^{LA4}/en^{LA7} mutant embryo. Pairs of segments are fused such that deep grooves are only observed every second segment (arrows). *f*, *g*, Higher magnification views of the periphery of the mutant in *d*. Grains are over every second segment over the deep grooves (arrows). Few or no grains are over the sites of the segment fusions. *h*, Dark-field micrograph of the ventral cuticle of an 18-h wild-type embryo. Note the mouthparts (M), eight abdominal denticle bands, and posterior spiracles (S). *i*, Dark-field micrograph of the ventral cuticle of an en^{LA4}/en^{SF31} embryo. Fused abdominal denticle belts are indicated. Scale bars, 50 μm in *a*–*e*; 25 μm in *f*, *g*; and 100 μm in *h*, *i*.

In 18 sections with intense labelling in bands 4 and 8 or 8 and 12, the strengths of the bands in the three-band interval between them varied such that the intervening odd-numbered bands were more intense than the even-numbered ones (Fig. 2*b*).

To document the order of appearance of these even-numbered bands, sections whose bands varied in intensity were examined. In 132 such embryo sections, pairs of even-numbered bands were compared and instances of clear differences in intensity were scored (Fig. 3). Band 2 was almost always more intense, and with only two exceptions, the more anterior bands were more intense than each of the posterior bands. As exceptions, the 8th was usually more intense than the 6th and the 12th more than the 10th (Fig. 3*a*, *b*). A pictorial representation of embryos with the implied four-segment periodic patterns is presented in order of increasing complexity and maturity (Fig. 3*c*, see also Figs 1*d*, 2*b*–*d*).

Even-numbered autoradiographic stripes increased in intensity throughout the 14th cycle. Between these were stripes with less intense signals. The resulting pattern, most prominent at the beginning of gastrulation, had a two-segment periodicity with alternating strong and weak autoradiographic signals over adjacent segments (Fig. 2*e*). The autoradiographic grains of the more intense even-numbered bands were dense over both the nuclear and cytoplasmic regions; in contrast the less intense odd-numbered bands were predominantly labelled over the nuclei.

The alternating pattern leads within minutes to an arrangement of stripes with equal intensity. The equalization process occurred with an anterior to posterior and a ventral to dorsal progression. As gastrulation proceeds, the ventral germ band extends around the posterior end onto the dorsal surface. In sections of germ band elongation embryos, additional bands of hybridization in the head and posterior regions were observed as reported previously[2]. By this stage, all of the stripes were two to three cells wide and were equally intense. Consistent with previous descriptions, cells expressing the *engrailed* locus were observed in the progenitors of the mesoderm and nervous system throughout the germ-band elongation stages. However, the improved preservation of sections and longer exposures revealed, in addition, expression in each segmental ganglion of the embryonic nervous system during later stages (Fig. 4*c*).

Expression of *fushi tarazu* in early embryos

Gene expression in a pattern with reiterated periodic bands was first described for the *fushi tarazu* locus[8]. To compare the processes that generate the patterns of *engrailed* and *ftz* expression, embryo sections were hybridized with a *ftz* probe in parallel to the experiments described above for the *engrailed* gene. Our results largely confirm the work of Hafen *et al.*[8], but reveal two additional intermediate stages in the temporal and spatial pattern of *ftz* expression—generally dispersed transcription at nuclear cycle 10 and a four-band stage early in cycle 14.

Localization of *ftz* RNA was first detected in syncytial blastoderm embryos during their 10th nuclear division cycle. Autoradiographic grains were localized over both yolk and

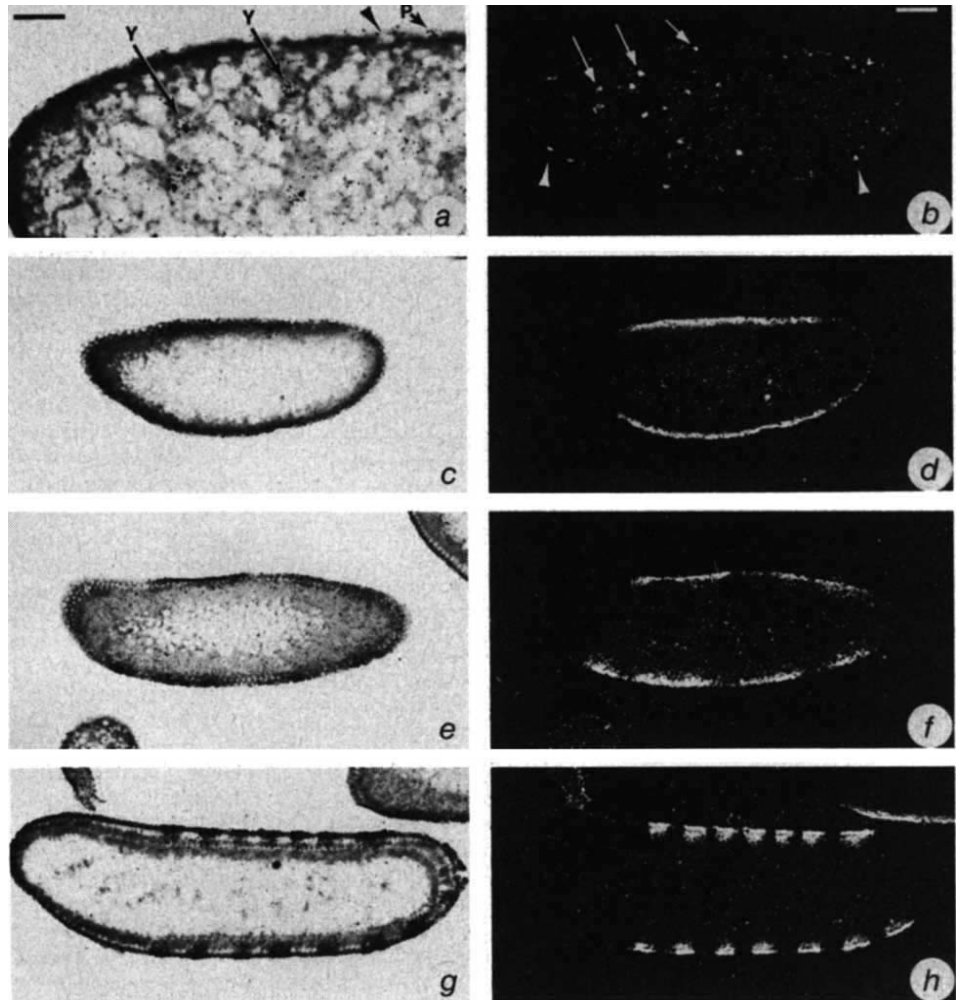

Fig. 5 Patterns of *fushi tarazu* transcripts in syncytial and cellular blastoderm stage embryos. *a, b, ftz* transcripts were detected over peripheral (P) and yolk nuclei (Y) at cycle 10 (arrows in *a* and *b*). The bright-field micrograph is a high-magnification image of the section shown in dark-field in *b*. Arrows point to corresponding nuclei. Arrowhead in *a* points to an unlabelled nucleus. Arrowheads in *b* point to examples of labelled peripheral nuclei. *c, d*, Embryo at cycle 12. During cycles 11–13, *ftz* transcript is evenly distributed over the middle portion at the edge of the embryo as previously reported[8]. *e, f*, Cycle-14 embryo; *ftz* transcripts are in four broad bands. *g, h*, Cycle-14 embryo with membrane furrows extended just beyond the nuclei; *ftz* transcripts are in seven bands. The probe was pDmV61H3.5 (a genomic 3.5 kilobase pair *Hin*dIII subclone in pUC8[29]), nick-translated with tritiated nucleotides. Scale bar, 25 μm in *a*, and 50 μm in *b–h*.

peripheral nuclei (Fig. 5*a, b*). Labelled nuclei were along the entire egg length, although not all peripheral nuclei were labelled. By the 12th cycle, *ftz* RNA was uniformly distributed in the cortical region of the embryo, from approximately 15% to 65% egg length (Fig. 5*c, d*). No further regional localization of the hybridizing RNA was observed until the 14th cycle, when autoradiographic grains were in discrete regions that approximate four broad bands (Fig. 5*e, f*). The most anterior band was not as wide as the others, but as the nuclei elongate and before the membrane furrows penetrate into the embryo, the three posterior broad stripes subdivided and yielded a pattern of seven discrete regions of hybridization (Fig. 5*g, h*). At both the four- and seven-band stages, the discrete gaps that define the bands appeared in an anterior-to-posterior and ventral-to-dorsal progression. There was no apparent difference in density of autoradiographic grains over the different stripes. In stage 14 embryos *ftz* transcripts were more numerous than *engrailed* as estimated from grain densities after *in situ* hybridization.

The existence of the transient four-band stage was documented by tabulating the order of appearance of gaps between hybridization stripes. With only three exceptions, the gaps defined the more anterior stripes first. These exceptions were: the gap between stripes 3 and 4 formed before the stripe 2–3 separation, and the gap between stripes 5 and 6 formed before the stripe 2–3 and stripe 4–5 separations (Fig. 6). Figure 6*c* summarizes the implied progression of *ftz* expression from uniform to banded distribution.

To establish the relationship between the stripes of *ftz* and *engrailed* hybridization and the segment primordia in the blastoderm, the repeat lengths of the various periodic patterns were compared. In sections of early stage 14 embryos in which the gaps between bands of *ftz* transcript were developing, the distance between gaps 1–2 and 3–4, and between gaps 3–4 and 5–6 was 88 ± 11 μm, corresponding to 13.8 ± 1.8 adjacent nuclei (56 measurements were taken). In sections of early stage 14 embryos hybridized with the *engrailed* probe, the distance between prominent bands 4 and 8, and between 8 and 12 was 92 ± 11 μm, corresponding to 14.4 ± 1.7 adjacent nuclei (46 measurements). Thus, the intervals of *engrailed* expression defined by bands 4, 8 and 12 have the same periodicity as the initial gaps of *ftz* expression. Given the estimated segment width of 3–4 cells[9], this periodicity corresponds to four segments. As described previously[2,3,8], later cycle 14 embryos with 14 stripes of *engrailed* and 7 stripes of *ftz* expression have periodicities that correspond to one and two segments, respectively.

Throughout the syncytial blastoderm and cellular blastoderm stages, the autoradiographic grains of *ftz* hydridization were most concentrated over the periplasmic region between the nuclei and the embryo cortex. This sequestration of *ftz* RNA contrasts with the more generally dispersed *engrailed* RNA and may suggest novel mechanisms for the regulation of RNA storage and utilization.

Transcript localization in *engrailed* embryos

All developmental stages[18,20–22] are affected by *engrailed* mutations. The *engrailed* cells in mosaic adults develop abnormally in all posterior compartments and generate similar types of defects in each segment[20–24]. Yet mutant embryos have fused pairs of segments, and very occasionally, fusions of groups of four segments (Fig. 4*h, i*)[22]. A gene such as *engrailed* that is

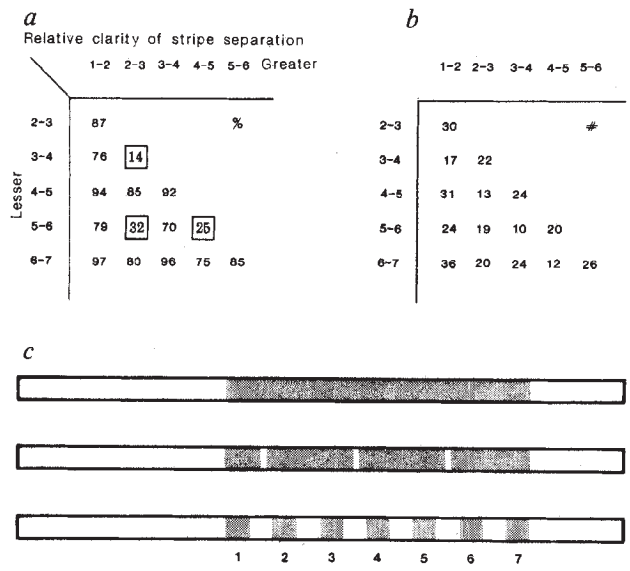

Fig. 6 The order of appearance of gaps in *ftz* expression along the embryo periphery was determined in 68 section edges from 34 sections. Sections chosen for analysis had gaps of varying clarity. For each comparison of two gaps, part *b* indicates the total number of cases with differences in the clarity of the gaps and part *a* indicates the percentages of such comparisons in which the gaps designated along the horizontal axis were more pronounced than the gaps on the vertical axis. The boxed figures indicate cases of posterior gaps becoming pronounced before anterior ones. *c*, A summary of the types of patterns observed. Embryos of increasing age are portrayed as rectangles with their posterior pole to the right. The dotted areas indicate regions of hybridization.

expressed in every segment might be expected to affect all segments similarly, whereas pairwise segment fusions might be expected in mutants of genes required in every second segment[25]. Thus the *engrailed* embryonic phenotype was surprising. We now demonstrate a direct correlation between the fusion phenotype of *engrailed* mutant embryos and the expression of the *engrailed* gene in periodic, two-segment-wide intervals.

Sections of *engrailed* mutant embryos were hybridized with the *engrailed* complementary DNA probe. Mutants examined were en^{LA4}/en^{LA7} heterozygotes (both apparent point mutations), and en^{C2} (an inversion breakpoint within the *engrailed* locus approximately 15 kilobase pairs upstream of the transcription unit (B. Drees and T.K., unpublished)) hemizygotes[22]. Mutants were identified in sections by their abnormal morphology and abnormal distribution of *engrailed* transcripts. Whereas in wild-type embryos the intensity of hybridization to the posterior compartment stripes alternated for a brief period in the cellular blastoderm and early gastrula and was uniform thereafter (Figs 2*f*, 4*a*, *c*, *e*), in most mutant embryos the alternating intensity persisted through germ-band elongation and germ-band shortening (Fig. 4*b*, *d*, *f*, *g*). The identities of the more prominent stripes in the mutant embryos corresponded with the location of the more intense stripes of hybridization of younger wild-type embryos; for example, the stripe at the posterior edge of the cephalic furrow was prominent in both (arrow in Fig. 4*b*). Comparison of the phasing of the alternating transcriptional pattern with the fused segment morphology of the mutants indicated that the weaker stripes of the alternating pattern coincide with the positions of the segment fusions (Fig. 4*d*, *f*, *g*).

Thus, apparent point mutations or breakpoint mutations upstream of the transcription unit both affect the spatial and temporal pattern of *engrailed* expression. This demonstrates that DNA 5′ to the transcription unit is involved in transcriptional regulation and that the *engrailed* function may modulate its own expression, either by directly affecting transcription or through interactions with other regulatory factors.

Discussion

The surface of the *Drosophila* cellular blastoderm is uniform in appearance, but its constituent cells are not equivalent. These studies and previous work[8] have shown that during the 14th nuclear division cycle, the blastoderm cells differentiate to express selected genes in remarkably precise patterns. Maturation of the expression patterns of the *engrailed* and *ftz* genes have provided two views of this differentiation process, a process that progressively subdivides the embryo into biochemically and spatially distinctive portions.

Apparent differences between the development of the *engrailed* and *ftz* patterns of expression include earlier maturation of the *ftz* pattern and contrasting modes for generating bands of expression: new bands of *engrailed* expressing nuclei seem to be added while *ftz*-expressing nuclei are suppressed in a patterned arrangement. However, direct comparisons between the patterns of *engrailed* and *ftz* RNA are made difficult by the lower abundance of the *engrailed* transcripts. The presence of *engrailed* transcripts in cleavage and syncytial blastoderm stages has been demonstrated by Northern analysis[18], but the low-level expression, which may be generally dispersed or distributed in a portion of the embryo, was not detectable with our *in situ* hybridization methods. The appearance of the *engrailed* patterns in *in situ* autoradiograms may be delayed until transcript levels are sufficient to be detected by our assay. Therefore, the great quantitative difference between levels of *ftz* and *engrailed* transcripts may mask fundamental similarities.

For both *engrailed* and *ftz*, the mature pattern of equally sized and equally spaced stripes of expressing cells emerges from patterns with longer repeat lengths that define fewer units. Maturation proceeds with anterior to posterior and ventral to dorsal polarities. For *ftz*, expression progressively narrows to four broad bands with a four-segment repeat length before dividing into seven narrower ones with a two-segment-repeat length. For *engrailed*, bands one to two cells wide define long intervals that shorten in a stepwise manner—first two bands (2 and 8 ventrally), then a four-segment periodicity, then two, and then in one-segment intervals.

That reiterated patterns of expression progress from longer to shorter repeat lengths suggests that the process of segmentation involves progressive partitioning of large units into smaller ones. The existence of discrete intermediate stages of segmentation has been proposed previously on theoretical grounds[26], and is strongly supported by the pattern of *engrailed* expression in *engrailed* mutants. Mutant late gastrulas had *engrailed* transcripts in patterns characteristic of younger embryos—in intervals greater than a single segment—indicating that the segmental fusions of *engrailed* mutants may be relics of earlier developmental units. A similar conclusion was drawn earlier from the phenotypes of the 'pair-rule' segmentation mutants that affect homologous portions of every second embryonic segment. It was suggested that such phenotypes are indicative of the transient existence of double-segment-sized units or fields[25].

The sequence in which the spacing of segments in the embryo is defined eliminates several possible mechanisms of segmentation. It indicates that the precisely spaced rows of cells in each segment are not designated in a simple sequential fashion at some predefined interval along the embryo's longitudinal axis. Nor do the many elements of the pattern appear simultaneously in their final form. Rather the mature pattern seems to involve proportioning of the embryo into successively smaller units. Such proportioning may provide the basis for coding position along the embryo's longitudinal axis. The overlapping activities of genes expressed with periodicities of one segment, two segments and larger intervals, together could direct in a combinatorial way the development of the blastoderm cells.

This work was supported by a fellowship from the Jane Coffin Childs Memorial Fund for Medical Research to M.P.W. and a NIH grant to T.K. We thank M. Scott for providing the *fushi tarazu* genomic clone, T. Karr and M. Simon for technical advice, and S. Poole and G. Martin for helpful comments on the manuscript.

Received 4 September; accepted 2 October 1985.

1. Garcia-Bellido, A. *Ciba Fdn Symp.* **29**, 161-182 (1975).
2. Kornberg, T., Siden, I., O'Farrell, P. & Simon, M. *Cell* **40**, 45-53 (1985).
3. Fjose, A., McGinnis, W. & Gehring, W. *Nature* **313**, 284-289 (1985).
4. Wieschaus, E. & Gehring, W. *Devl Biol.* **50**, 249-263 (1976).
5. Lawrence, P. & Morata, G. *Devl Biol.* **56**, 40-51 (1977).
6. Steiner, E. *Wilhelm Roux Arch. EntwMech.* **180**, 9-30 (1976).
7. Wakimoto, B. & Kaufman, T. *Devl Biol.* **81**, 51-64 (1981).
8. Hafen, E., Kuroiwa, A. & Gehring, W. *Cell* **37**, 833-841 (1984).
9. Lohs-Schardin, M., Cremer, C. & Nusslein-Volhard, C. *Devl Biol.* **73**, 239-255 (1979).
10. Rabinowitz, M. *J. Morph.* **69**, 1-49 (1941).
11. Sonnenblick, B. in *Biology of Drosophila* (ed. Demerec, M.) 62-167 (Wiley, New York, 1950).
12. Zalokar, M. & Erk, I. *J. Microsc. Biol. Cell* **25**, 97-106 (1976).
13. Turner, F. & Mahowald, A. *Devl Biol.* **50**, 95-108 (1976).
14. Foe, V. & Alberts, B. *J. Cell Sci.* **61**, 31-70 (1983).
15. Fullilove, S. & Jacobson, A. *Devl Biol.* **26**, 560-577 (1971).
16. Zalokar, M. *Devl Biol.* **49**, 425-427 (1976).
17. Lamb, M. & Laird, C. *Devl Biol.* **52**, 31-42 (1976).
18. Karr, T., Ali, Z., Drees, B. & Kornberg, T. *Cell* (in the press).
19. Underwood, E., Turner, F. & Mahowald, A. *Devl Biol.* **74**, 286-301 (1980).
20. Garcia-Bellido, A. & Santamaria, P. *Genetics* **72**, 87-104 (1972).
21. Lawrence, P. & Morata, G. *Devl Biol.* **50**, 321-337 (1976).
22. Kornberg, T. *Proc. natn. Acad. Sci. U.S.A.* **78**, 1095-1099 (1981).
23. Kornberg, T. *Devl Biol.* **86**, 363-372 (1981).
24. Lawrence, P. & Struhl, G. *EMBO J.* **1**, 827-833 (1982).
25. Nusslein-Volhard, C. & Wieschaus, E. *Nature* **287**, 795-801 (1980).
26. Kauffman, S., Shymko, R. & Trabert, K. *Science* **199**, 259-270 (1978).
27. Mitchison, T. & Sedat, J. *Devl Biol.* **99**, 261-264 (1983).
28. Lawrence, P. & Johnston, P. *EMBO J.* **3**, 2839-2844 (1984).
29. Laughon, A. & Scott, M. *Nature* **310**, 24-31 (1984).

Transcription pattern of the *Drosophila* segmentation gene *hairy*

P. W. Ingham, K. R. Howard & D. Ish-Horowicz

Developmental Genetics Laboratory, Imperial Cancer Research Fund, Mill Hill Laboratories, Burtonhole Lane, London NW7 1AD, UK*

Segmentation of the Drosophila *embryo requires expression of the pair-rule genes, mutations of which cause reiterated deletions in alternate segments along the antero-posterior body axis. We find that transcripts of one such gene,* hairy, *accumulate in eight distinct regions of the early embryo. This pattern of expression is compared with that of another pair-rule gene,* fushi tarazu, *and its dependence on maternally expressed genes is described.*

A COMMON theme in the organization of many metazoa is the subdivision of the body into a series of homologous segments[1]. Different structures are then elaborated in the various segments to generate complex forms. A vivid example of such segmental or metameric organization is provided by the insects. Although segmentation of the insect body has been studied for many years[2-4], the prospect of an understanding at the molecular level has only recently come into view with the identification, in *Drosophila melanogaster*, of most of the genes required for the process[5-9].

Metameric organization is established during early *Drosophila* embryogenesis[10-12] as the incipient cells of the blastoderm embryo respond to information generated epigenetically in the maternally derived environment of the egg[13,14]. This response depends on the expression of the zygotic genome and, in particular of genes defined by a class of zygotically acting mutations[5-8] which disrupt the generation of the normal segmental pattern. These fall into three distinct phenotypic classes: (1) the gap mutations, which cause the deletion of contiguous groups of segments, (2) the pair-rule mutations, which result in deletions of homologous pattern elements in alternate segments, and (3) the segment polarity mutations, which affect the patterning of every segment.

The discovery of the pair-rule class provided the first evidence of a double-segment order during the formation of the metameric pattern[5]. This order is reflected at the molecular level by the pattern of expression[15] of the pair-rule gene *fushi tarazu* (*ftz*)[16,17]. At the blastoderm stage, *ftz* transcripts accumulate in seven discrete regions which repeat along the antero-posterior axis of the embryo with double-segment periodicity[15]. Such a precise pattern of transcript distribution implies that the ftz^+ function is specifically required for the establishment of particular metameric units—those which are deleted in ftz^- mutants. Mutants of a second pair-rule gene, *hairy*(*h*)[5,18], cause a pattern of deletions which is approximately complementary to that typical of *ftz*, suggesting a corresponding complementarity of spatial expression and function.

We have analysed the spatial distribution of *h* RNA in early embryos, and compare it with the previously described *ftz* transcription pattern. We also show that establishment of the *h* transcription pattern depends on maternal determinants of both antero-posterior and dorso-ventral polarity.

Effect of *hairy* on embryonic segmentation

The metameric organization of the *Drosophila* body is directly reflected in the cuticle of the first-instar larva. This is especially clearly illustrated by the pattern on its ventral surface (Fig. 1 and ref. 19). Each thoracic and abdominal segment secretes a characteristic belt of cuticular processes or denticles. The metameric origin of the mouthparts is obscured by head involution, but cuticular structures characteristic of each segment can be easily identified.

Larvae homozygous for *h* null mutations exhibit a range of segmentation defects[18] representing variations on a common theme, the pair-rule phenotype. The most regular *h* phenotype (Fig. 1*c*) consists of the deletion of the anterior region of each even-numbered abdominal segment and the posterior region of each odd-numbered abdominal segment from the larval cuticular pattern. This is almost the precise complement of the phenotype characteristic of amorphic alleles of the pair-rule gene *ftz* (Fig. 1*d*). In both cases, the same register of deletions extends into the thoracic and head segments (Fig. 1*a*). In *h* mutants, structures which derive from the mandibular (G1) and labial (G3) segments (the ventral arms of the cephalopharyngeal skeleton and H-piece respectively)[20] are deleted. In addition the medial tooth, a derivative of the labrum, is disrupted. This contrasts with the phenotype of strong *ftz* alleles in which only derivatives of the post-oral maxillary and labial segments are affected.

This regular pair-rule phenotype is typical only of a proportion of animals homozygous for any given amorphic *h* allele[18]. Commonly, more extreme defects are seen. The entire third thoracic segment is often deleted such that the second thoracic and first abdominal dentical bands fuse; similarly the remaining three posterior abdominal bands frequently fuse to form a continuous 'lawn' of denticles exhibiting polarity perturbation[18,21].

These lesions in the larval cuticle are manifestations of defects occurring much earlier during embryogenesis. Absence of h^+

* New address from December 1985: ICRF Developmental Biology Unit, Department of Zoology, University of Oxford, South Parks Road, Oxford OX1 3PS, UK.